Statistica Sinica **31** (2021), 1397-1414
doi:https://doi.org/10.5705/ss.202018.0468

# SPARSE DEEP NEURAL NETWORKS USING $L_{1,\infty}$-WEIGHT NORMALIZATION

Ming Wen[1], Yixi Xu[2], Yunling Zheng[1], Zhouwang Yang[1] and Xiao Wang[2]

[1] *University of Science and Technology of China and* [2] *Purdue University*

*Abstract:* Deep neural networks (DNNs) have recently demonstrated an excellent performance on many challenging tasks. However, overfitting remains a significant challenge in DNNs. Empirical evidence suggests that inducing sparsity can relieve overfitting, and that weight normalization can accelerate the algorithm convergence. In this study, we employ $L_{1,\infty}$ weight normalization for DNNs with bias neurons to achieve a sparse architecture. We theoretically establish the generalization error bounds for both regression and classification under the $L_{1,\infty}$ weight normalization. Furthermore, we show that the upper bounds are independent of the network width and the $\sqrt{k}$-dependence on the network depth $k$, which are the best available bounds for networks with bias neurons. These results provide theoretical justifications for using such weight normalization to reduce the generalization error. We also develop an easily implemented gradient projection descent algorithm to practically obtain a sparse neural network. Finally, we present various experiments that validate our theory and demonstrate the effectiveness of the resulting approach.

*Key words and phrases:* Deep neural networks, generalization, overfitting, rademarcher complexity, sparsity.

## 1. Introduction

Deep neural networks (DNNs) have recently attracted attention as a result of several successful real-world applications (Goodfellow et al. (2016)). On the one hand, advancements in stochastic gradient descent (SGD) and graphical processing units (GPUs) have made it possible to scale DNN training to millions of parameters (Krizhevsky, Sutskever and Hinton (2012); Jaderberg et al. (2015); Szegedy et al. (2015)). On the other hand, overfitting is a significant problem in DNNs, leading to poor generalization. Recent works (Han, Mao and Dally (2016); Louizos, Ullrich and Welling (2017); Molchanov, Ashukha and Vetrov (2017)) have shown that the networks can be pruned significantly without loss in accuracy. At the same time, other methods have been developed to address the issue of overfitting, including early stopping, weight penalties such as $L_1$

Corresponding author: Yixi Xu, Department of Statistics, Purdue University, West Lafayette, IN 47907, USA. E-mail: xu573@purdue.edu.

and $L_2$ regularizations, weight sharing (Nowlan and Hinton (1992)), and dropout (Srivastava et al. (2014)).

Empirical evidence suggests that inducing sparsity can relieve overfitting and save computation resources. A common strategy is to apply a sparsity-inducing regularizer such as the $L_0$ penalty (Louizos, Welling and Kingma (2018)) or the total number of parameters in the network (Srinivas, Subramanya and Babu (2017)). However, few theoretical investigations or justifications on sparse DNNs appear in the literature.

Weight normalization, by bounding the Euclidean norm of the incoming weights of each unit, has been shown to accelerate the convergence of SGD optimization across many applications (Salimans and Kingma (2016)). As such, we employ weight normalization and induce sparsity by bounding the $L_{1,\infty}$ norm of the weight matrix (including bias) for each layer. By doing so, we induce sparsity in a systematic way. Furthermore, we have developed capacity control for such models. We show that the generalization error upper bounds are independent of the network width and the $\sqrt{k}$-dependence on the depth $k$ of the network, which are the best available bounds for networks *with bias neurons*. Our results provide theoretical justifications for using weight normalization, which leads to a sparse DNN. At the same time, the generalization error has minimal dependence on the network architecture. $L_{1,\infty}$ norm-constrained fully connected DNNs *without bias neurons* have been investigated in prior studies (Bartlett (1998); Neyshabur, Tomioka and Srebro (2015); Sun et al. (2016); Golowich, Rakhlin and Shamir (2018)). The Rademacher complexity bounds in (Bartlett (1998); Neyshabur, Tomioka and Srebro (2015); Sun et al. (2016)) are $2^k$ times larger than our result in Theorem 1, even without the bias neurons in each hidden layer. Furthermore, it is difficult to extend the work of (Golowich, Rakhlin and Shamir (2018)) to include fully connected DNNs with bias neurons, especially when the activation function, such as the tanh activation function, fails to map the bias neuron to one. As a comparison, our result is applicable to all Lipschitz-continuous activation functions.

This study contributes to the literature in three ways. First, we theoretically establish the generalization error bounds for both regression and classification under $L_{1,\infty}$ weight normalization for networks *with bias neurons*. Second, we develop an easily implemented gradient projection descent algorithm to practically obtain a sparse neural network. Third, we perform various experiments to validate our theory and demonstrate the effectiveness of the resulting approach.

The remainder of the paper is organized as follows. In Section 2, we define sparse DNNs. Section 3 gives the Rademacher complexities, the generalization

bounds for both regression and classification. In Section 4, we propose a gradient projection descent algorithm. Section 5 includes both synthetic and real-world experiments that validate our theoretical findings.

## 2. The Model

In this section, we define the general prediction problem and introduce sparse DNNs.

### 2.1. The general prediction problem

Assume that $\boldsymbol{x}_1, \ldots, \boldsymbol{x}_n$ are $n$ independent random variables on $\mathcal{X} \subseteq \mathbb{R}^{m_1}$, $\boldsymbol{z}_1, \ldots, \boldsymbol{z}_n$ are on $\mathcal{Z} \subseteq \mathbb{R}^{m_2}$, $y_1, \ldots, y_n$ are on $\mathcal{Y} \subseteq \mathbb{R}$, and the noise $\varepsilon_1, \ldots, \varepsilon_n$ are independent, while satisfying that $\mathbb{E}(\varepsilon_i) = 0$. The general prediction problem is defined as

$$\begin{aligned} \boldsymbol{z}_i &= f(\boldsymbol{x}_i) + \varepsilon_i \\ y_i &= t(\boldsymbol{z}_i), \end{aligned} \tag{2.1}$$

where $t : \mathcal{Z} \to \mathcal{Y}$ is a fixed function related to the prediction problem, and $f : \mathcal{X} \to \mathcal{Z}$ is an unknown function. We provide two examples to show how to adapt equation (2.1) to different settings. For a regression, we have $m_2 = 1$, $\mathcal{Z} = \mathcal{Y}$, and $t(z) = z$. For a classification, we can define $m_2$ as the number of classes, $\mathcal{Y} = \{1, 2, \ldots, m_2\}$, and $t = \text{argmax}$.

### 2.2. Overfitting

We first provide a formal definition of overfitting. Let $L(f(\cdot), \cdot) : \mathcal{X} \times \mathcal{Y} \to \mathbb{R}$ be the loss function. Define the expected and empirical risks, respectively, as

$$\mathbb{E}_L(f) = \mathbb{E}_{(\boldsymbol{x},y)\sim\mathcal{D}}[L(f(\boldsymbol{x}), y)], \quad \widehat{\mathbb{E}}_L(f) = \frac{1}{n}\sum_{i=1}^{n} L(f(\boldsymbol{x}_i), y_i),$$

where $\mathcal{D}$ is the underlying distribution of $(\boldsymbol{x}, y)$. In practice, the empirical risk corresponds to the training error, and the expected risk corresponds to the testing error. In general, a learning algorithm is said to *overfit* if it is more accurate in fitting known data, but less accurate in predicting new data. Mathematically, the difference between the expected risk and the empirical risk, called *generalization error*, is a measure of how accurately an algorithm is able to predict outcome values for previously unseen data. Let

$$\mathcal{E}_L(f) = \Big| \mathbb{E}_L(f) - \widehat{\mathbb{E}}_L(f) \Big|.$$

The performance of a DNN relies on the balance between the empirical risk and the generalization error. On the one hand, complex structures usually overfit the data, while achieving a low empirical risk. On the other hand, simple models generalize well, but might underfit the data. In practice, it is common to use a neural net with billions of parameters (e.g., Simonyan and Zisserman (2015)), with the training error even reducing to zero in many cases. Thus, we focus on the generalization error only.

Our goal is to control the generalization error $\mathcal{E}_L(f)$, making it less sensitive to the network architecture when adopting a DNN model. This generalization error bound can be studied using the *Rademacher complexity* and the techniques in Mohri, Rostamizadeh and Talwalkar (2012). Under some mild conditions, it is sufficient to bound the Rademacher complexity in order to control the generalization error. Here, we establish non-asymptotic uniform error bounds for $\mathcal{E}_L(f)$ when $f$ is a sparse DNN. These bounds have minimal dependence on the network structure.

### 2.3. Sparse DNNs

We begin with some notation for fully connected neural networks. A neural network on $\mathbb{R}^{d_0} \to \mathbb{R}^{d_{k+1}}$ with $k$ hidden layers is defined by a set of $k+1$ affine transformations $T_1 : \mathbb{R}^{d_0} \to \mathbb{R}^{d_1}, T_2 : \mathbb{R}^{d_1} \to \mathbb{R}^{d_2}, \ldots, T_{k+1} : \mathbb{R}^{d_k} \to \mathbb{R}^{d_{k+1}}$ and an activation function $\sigma$. In this paper, we consider activation functions satisfying $\sigma(0) = 0$. Note that this condition holds for widely used activation functions, including ReLU and tanh. The affine transformations are parameterized by $T_\ell(\mathbf{u}) = \boldsymbol{W}_\ell^T \mathbf{u} + \mathbf{B}_\ell$, where $\boldsymbol{W}_\ell \in \mathbb{R}^{d_{\ell-1} \times d_\ell}$ and $\mathbf{B}_\ell \in \mathbb{R}^{d_\ell}$, for $\ell = 1, \ldots, k+1$. The function represented by this neural network is

$$f(x) = T_{k+1} \circ \sigma \circ T_k \circ \cdots \circ \sigma \circ T_1 \circ \boldsymbol{x}.$$

Before introducing sparse DNNs, we build an augmented layer for each hidden layer by appending the bias neuron 1 to the original layer, and then combining the weight matrix and the bias vector to form a new matrix. We define the first hidden layer as

$$f_1(\boldsymbol{x}) = T_1 \circ \boldsymbol{x} \triangleq \langle \tilde{\mathbf{V}}_1, (1, \boldsymbol{x}^T)^T \rangle,$$

where $\tilde{\mathbf{V}}_1 = (\mathbf{B}_1, \boldsymbol{W}_1^T)^T \in \mathbb{R}^{(d_0+1) \times d_1}$.

Sequentially, for $\ell = 2, \ldots, k$, define the $\ell$th hidden layer as

$$f_\ell(\boldsymbol{x}) = T_\ell \circ \sigma \circ f_{\ell-1}(\boldsymbol{x}) \triangleq \langle \tilde{\mathbf{V}}_\ell, (1, \sigma \circ f_{\ell-1}^T(\boldsymbol{x}))^T \rangle,$$

where $\tilde{\mathbf{V}}_\ell = (\mathbf{B}_\ell, \boldsymbol{W}_\ell^T)^T \in \mathbb{R}^{(d_{\ell-1}+1)\times d_\ell}$. The output layer is

$$f(\boldsymbol{x}) = T_{k+1} \circ \sigma \circ f_k(\boldsymbol{x}) \triangleq \langle \tilde{\mathbf{V}}_{k+1}, (1, \sigma \circ f_k^T(\boldsymbol{x}))^T \rangle,$$

where $\tilde{\mathbf{V}}_{k+1} = (\mathbf{B}_{k+1}, \boldsymbol{W}_{k+1}^T)^T \in \mathbb{R}^{(d_k+1)\times d_{k+1}}$.

The sparsity of the DNN is controlled by setting proper constraints for the $L_{1,\infty}$ norm of each hidden layer, where the $L_{1,\infty}$ norm of a $s_1 \times s_2$ matrix $A$ is defined as

$$\|A\|_{1,\infty} = \max_j \left( \sum_{i=1}^{s_1} |a_{ij}| \right).$$

Specifically, define $\mathcal{SN}_{c,\boldsymbol{o}}^{k,\boldsymbol{d},\sigma}$ as the collection of all sparse DNNs $f(\boldsymbol{x}) = T_{k+1} \circ \sigma \circ T_k \circ \cdots \circ \sigma \circ T_1 \circ \boldsymbol{x}$ satisfying the following:

(a) It has $k$ hidden layers.

(b) The number of neurons in the $\ell$th hidden layer is $d_\ell$, for $\ell = 1, 2, \ldots, k$. The dimension of the input is $d_0$, and that of the output is $d_{k+1}$.

(c) $\|T_\ell\|_{1,\infty} \triangleq \|\tilde{\mathbf{V}}_\ell\|_{1,\infty} \le c$, for $\ell = 1, \ldots, k$.

(d) The $L_1$ norm of the $j$th column of $\tilde{\mathbf{V}}_{k+1}$ is bounded by the $j$th element of $\boldsymbol{o}$: $\|\tilde{\mathbf{V}}_{k+1}[\cdot, j]\|_1 \le o_j$ for $j = 1, \ldots, d_{k+1}$.

We call $c$ the normalization constant in the rest of the paper. Furthermore, define the collection of sparse DNNs without any constraint on the output layer as

$$\mathcal{S}_c^{k,\boldsymbol{d},\sigma} = \bigcup_{\boldsymbol{o} \ge \mathbf{0}} \mathcal{SN}_{c,\boldsymbol{o}}^{k,\boldsymbol{d},\sigma}.$$

In order to obtain a sparse neural network, we need to transform our understanding of a problem into a loss function $L(\cdot, \cdot)$. Then, it is equivalent to solving the optimization problem

$$\min_f \left\{ \sum_{i=1}^n L(f(\boldsymbol{x}_i), y_i) \,\middle|\, f \in \mathcal{S}_c^{k,\boldsymbol{d},\sigma} \right\}, \tag{2.2}$$

where $(\boldsymbol{x}_1, y_1), \ldots, (\boldsymbol{x}_n, y_n) \in \mathbb{R}^{m_1 \times 1}$ are samples, $k$ and $\boldsymbol{d}$ define the depth and width, respectively, of the DNN, and the normalization constant $c$ controls the sparsity. We focus on the influence of $c$ on the generalization behavior and sparsity of the DNN, and provide generalization bounds for sparse DNNs with unconstrained output layers.

## 3. The Learning Theory

In this section, assume that $\mathcal{X} = [-1, 1]^{m_1}$ and the activation function $\sigma$ is $\rho_\sigma$-Lipschitz continuous. Note that ReLU and tanh are both 1-Lipschitz continuous.

### 3.1. Rademacher complexities

The *empirical Rademacher complexity* of the hypothesis class $\mathcal{F}$ with respect to a data set $S = \{z_1 \dots z_n\}$ is defined as

$$\widehat{\mathfrak{R}}_S(\mathcal{F}) = \mathbb{E}_\epsilon \left[ \sup_{f \in \mathcal{F}} \left( \frac{1}{n} \sum_{i=1}^{n} \epsilon_i f(z_i) \right) \right],$$

where $\epsilon = \{\epsilon_1 \dots \epsilon_n\}$ are $n$ independent Rademacher random variables. The *Rademacher complexity* of the hypothesis class $\mathcal{F}$ with respect to $n$ samples is defined as

$$\mathfrak{R}_n(\mathcal{F}) = \mathbb{E}_{S \sim \mathcal{D}^n} \left[ \widehat{\mathfrak{R}}_S(\mathcal{F}) \right].$$

In the following theorem, we bound the Rademacher complexity of $\mathcal{SN}_{c,o}^{k,\boldsymbol{d},\sigma}$ when the output dimension is one. This is used later to obtain the generalization bounds for both regression and classification.

**Theorem 1.** *Fix the depth $k \geq 0$, the normalization constant $c > 0$, the output layer constraint $o > 0$, the widths $d_\ell \in \mathbb{N}_+$, for $\ell = 1, \dots, k$, and $d_{k+1} = 1$. Then for any set $S = \{\boldsymbol{x}_1, \dots, \boldsymbol{x}_n\} \subseteq \mathcal{X}$ , we have*

$$\widehat{\mathfrak{R}}_S(\mathcal{SN}_{c,o}^{k,\boldsymbol{d},\sigma}) \leq o\sqrt{\frac{(k+1)\log 16}{n}} \left( \sum_{\ell=0}^{k} (c\rho_\sigma)^\ell + (c\rho_\sigma)^k \right) + o(c\rho_\sigma)^k \sqrt{\frac{2\log(2m_1)}{n}}.$$

*Furthermore, if $c\rho_\sigma \geq 1$,*

$$\widehat{\mathfrak{R}}_S(\mathcal{SN}_{c,o}^{k,\boldsymbol{d},\sigma}) \leq \frac{1}{\sqrt{n}} o(c\rho_\sigma)^k (\sqrt{(k+3)\log 4} + \sqrt{2\log(2m_1)}).$$

**Remark 1.** When $\log(m_1)$ is small, we briefly summarize the dependence of the above bound on $k$ under different choices of $c$:

- $c\rho_\sigma < 1$: $O(\sqrt{k}((1 - (c\rho_\sigma)^{k+1})/(1 - c\rho_\sigma)))$
- $c\rho_\sigma \geq 1$: $O(\sqrt{k}(c\rho_\sigma)^k)$.

The complexity bound does not depend on the width of the network. In addition to the product of the $L_{1,\infty}$ norms of each layer, the complexity bound depends

on the depth $k$ by $O(\sqrt{k})$ when $c\rho_{\sigma} < 1$, and $\sqrt{k}(c\rho_{\sigma})^k$ otherwise.

### 3.2. Generalization bounds for regression

In this section, consider a specific case of equation (2.1), where $t$ is an identity transformation, and $m_2 = 1$. Assume the following conditions in this section:

(A1). $(\boldsymbol{x}, y)$ is a random variable of support $\mathcal{X} \times \mathcal{Y}$ and distribution $\mathcal{D}$, and $S = \{(\mathbf{x}_i, y_i)\}_{i=1}^n$ is a data set of $n$ independent and identically distributed (i.i.d.) samples drawn from $\mathcal{D}$.

(A2). The normalization constant $c > 0$, the number of hidden layers $k \in [0, \infty)$, and the widths $\boldsymbol{d} \in \mathbb{N}_+^{k+2}$, with $d_0 = m_1$ and $d_{k+1} = 1$.

(A3). The loss function $L(f(\boldsymbol{x}), y)$ is 1-Lipschitz continuous on its first argument. In addition, $|L(f(\boldsymbol{x}), y)| \leq 1$.

The following theorem shows the generalization bound that holds uniformly for any sparse DNN in $\mathcal{S}_c^{k,\boldsymbol{d},\sigma}$. Note that the sample $S = \{(\mathbf{x}_i, y_i)\}_{i=1}^n$ is a data set randomly drawn from $\mathcal{D}$, and that the following statement holds with high probability over the choice of the sample $S$.

**Theorem 2.** *Assume Conditions* (A1)–(A3) *hold and* $c\rho_{\sigma} \geq 1$. *Fix* $\delta \in (0, 1)$. *Then, with probability at least* $1 - \delta$ *over the choice of the sample* $S$, *for* **every** *sparse DNN* $f_T \in \mathcal{S}_c^{k,\boldsymbol{d},\sigma}$, *we have*

$$\begin{aligned}\mathcal{E}_L(f_T) \leq & \sqrt{\frac{\log(2/\delta) + 2\log(\|T_{k+1}\|_1 + 2)}{2n}} + \\ & \frac{2}{\sqrt{n}}(\|T_{k+1}\|_1 + 1)(c\rho_{\sigma})^k(\sqrt{(k+3)\log 4} + \sqrt{2\log(2m_1)}).\end{aligned} \tag{3.1}$$

**Remark 2.** The upper bound is a summation of $\sqrt{\log(2/\delta)+2\log(\|T_{k+1}\|_1+2)/2n}$ and $(2/\sqrt{n})(\|T_{k+1}\|_1 + 1)(c\rho_{\sigma})^k(\sqrt{(k+3)\log 4} + \sqrt{2\log(2m_1)})$. Both terms depend on the sample size $n$ by $n^{-1/2}$. Note that the $L_1$ norm of the output layer $\|T_{k+1}\|_1$ is data-dependent. In addition, the first term depends on the probability $1 - \delta$ by $\sqrt{\log(1/\delta)}$. The second term depends on the depth by $\sqrt{k}(c\rho_{\sigma})^k$, and the input dimension by $\sqrt{\log m_1}$. The case when $c\rho_{\sigma} < 1$ is discussed in the Supplementary Material.

**Remark 3.** Define the truncated mean squared error and the truncated mean absolute error by

$$L_S(f(\boldsymbol{x}), y) = \min\left(\left(\frac{y - f(\boldsymbol{x})}{2}\right)^2, 1\right)$$

and

$$L_A(f(\boldsymbol{x}), y) = \min\left(|y - f(\boldsymbol{x})|, 1\right),$$

respectively. It is easy to verify that both loss functions satisfy Condition (A3). Thus, we can apply Theorem 2 to both cases.

**Remark 4.** Condition (A3) is not always met in practice. It can be relaxed by assuming that the loss function $L(f(\boldsymbol{x}), y)$ is $B_0$-Lipschitz continuous on its first argument and $|L(f(\boldsymbol{x}), y)| \leq B_0$, where $B_0$ is a constant. The generalization error can still be bounded by applying Theorem 2 to the loss function $L/B_0$.

### 3.3. Generalization bounds for classification

In this section, we consider the case of equation (2.1) when $t = \text{argmax}$ and $\mathcal{Y} = \{1, 2, \ldots, m_2\}$. In the rest of the paper, we define the $j$th element of a vector $\mathbf{z}$ by $z[j]$. In this subsection, assume the following conditions:

(B1). $(\boldsymbol{x}, y)$ is a random variable of support $\mathcal{X} \times \mathcal{Y}$ and distribution $\mathcal{D}$, and $S = \{(\mathbf{x}_i, y_i)\}_{i=1}^n$ is a data set of $n$ i.i.d. samples drawn from $\mathcal{D}$.

(B2). The normalization constant $c > 0$, the number of hidden layers $k \in [0, \infty)$, and the widths $\boldsymbol{d} \in \mathbb{N}_+^{k+2}$, with $d_0 = m_1$ and $d_{k+1} = m_2$.

The cross-entropy loss function is defined as

$$L_C(f(\boldsymbol{x}), y) = -\log \frac{\exp(f(\boldsymbol{x})[y])}{\sum_j \exp f(\boldsymbol{x})[j]}.$$

We extend this to sparse DNNs with unconstrained output layers. For any transformation $T(\mathbf{u}) = V^T(1, \mathbf{u}^T)^T$, define $T[j]$ as $V[, j]$: the $j$th column of $V$.

**Theorem 3.** *Assume Conditions* (B1)–(B2) *hold and* $c\rho_{\boldsymbol{\sigma}} \geq 1$. *Fix* $\delta \in (0, 1)$. *Then, with probability at least* $1 - \delta$ *over the choice of* $S$, *every* $f_T \in \mathcal{S}_c^{k,\boldsymbol{d},\boldsymbol{\sigma}}$ *satisfies that*

$$\mathcal{E}_{L_C}(f_T) \leq O\left(\frac{(c\rho_{\boldsymbol{\sigma}})^k}{\sqrt{n}} \|T_{k+1}\|_{1,\infty} \left[\sqrt{\log \frac{1}{\delta}} + \frac{\|T_{k+1}\|_{1,1}}{\|T_{k+1}\|_{1,\infty}} \sqrt{m_2}(\sqrt{k} + \sqrt{\log m_1})\right]\right), \tag{3.2}$$

*where* $\|T\|_{1,1} = \sum_i \sum_j |v_{ij}|$, *if* $T(x) = \langle \mathbf{V}, (1, \boldsymbol{x}) \rangle$.

**Remark 5.** The upper bound is the product of $(c\rho_{\boldsymbol{\sigma}})^k \|T_{k+1}\|_{1,\infty} / \sqrt{n}$ and

$$\sqrt{\log \frac{1}{\delta}} + \frac{\|T_{k+1}\|_{1,1}}{\|T_{k+1}\|_{1,\infty}} \sqrt{m_2}(\sqrt{k} + \sqrt{\log m_1}).$$

**Algorithm 1** Gradient Projection Descent Algorithm

In each iteration:
**Input:** $\tilde{\mathbf{V}}^{(t)} = (\tilde{\mathbf{V}}_1^{(t)}, \ldots, \tilde{\mathbf{V}}_k^{(t)})$
**for all** $\ell = 1, \ldots, k$ **do**
  $\tilde{\mathbf{V}}_\ell^{(t+1)} := \tilde{\mathbf{V}}_\ell^{(t)} - \gamma_t \nabla L(\tilde{\mathbf{V}}_\ell^{(t)})$,
  where $\gamma_t$ is the stepsize at iteration $t$
  **for all** columns $\boldsymbol{v}$ in $\mathbf{V}_\ell^{(t+1)}$ **do**
    **if** $\|\boldsymbol{v}\|_1 > c$ **then**
      $\boldsymbol{v} = \text{proj}_{\|\cdot\|_1 \le c} \boldsymbol{v}$ by **Algorithm 2**
    **end if**
  **end for**
**end for**
**Output:** $\tilde{\mathbf{V}}^{(t+1)} = (\tilde{\mathbf{V}}_1^{(t+1)}, \ldots, \tilde{\mathbf{V}}_k^{(t+1)})$

**Algorithm 2** Projection to $L_1$ norm ball (Duchi et al. (2008))

**Input:** $\boldsymbol{v} \in \mathbb{R}^s$, $c$
Sort abs($\boldsymbol{v}$) into $\mu : \mu_1 \geqslant \mu_2 \geqslant \cdots \geqslant \mu_s$
Find $p^* = \max\{p \in [s] : \mu_p - (1/p)(\sum_{q=1}^{p} \mu_q - c) > 0\}$
Define $\theta = (1/p^*)(\sum_{q=1}^{p^*} \mu_q - c)$
**Output:** $\boldsymbol{w}$ s.t. $\boldsymbol{w}_p = \text{sgn}(\boldsymbol{v}_p) \cdot \max\{\text{abs}(\boldsymbol{v}_p) - \theta, 0\}$

The first term includes $(c\rho_{\sigma})^k \|T_{k+1}\|_{1,\infty}$, which reflects the range of the neural network $f_T$. The second term is the summation of $\sqrt{\log 1/\delta}$ and $\|T_{k+1}\|_{1,1}/\|T_{k+1}\|_{1,\infty}\sqrt{m_2}(\sqrt{k} + \sqrt{\log m_1})$, where $1-\delta$, $k$, $m_1$, and $m_2$ are the probability, depth, input dimension, and number of classes, respectively. The case when $c\rho_{\sigma} < 1$ is discussed in the Supplementary Material. Under this assumption, the generalization bound relies on $c\rho_{\sigma}$ by $O((1-(c\rho_{\sigma})^{k+1})/(1-c\rho_{\sigma}))$.

Our theoretical results can be easily extended to convolutional neural networks (CNNs), because a CNN can be viewed as a neural net with a sparse structure. Note that our generalization bound is independent of the widths of the neural network. When applying our results to CNNs, the bound does not depend on the number of kernels, which could number in the thousands in practice. In addition, it would be interesting to extend our theoretical results to residual neural networks.

## 4. The Algorithm

In this section, we propose a gradient projection descent algorithm to solve the optimization problem given in equation (2.2).

Recall that for a neural network $f(x) = T_{k+1} \circ \sigma \circ T_k \circ \cdots \circ \sigma \circ T_1 \circ \boldsymbol{x}$ with

$T_\ell(\mathbf{u}) = \tilde{\mathbf{V}}_\ell^T(1, \mathbf{u}^T)^T$, we have $f \in \mathcal{S}_c^{k,\boldsymbol{d},\sigma}$ if and only if

$$\left\|\tilde{\mathbf{V}}_\ell\right\|_{1,\infty} \leq c \quad \forall \ell \quad \text{or} \quad \left\|\tilde{\mathbf{V}}_\ell[\cdot, j]\right\|_1 \leq c \quad \forall\, \ell, j.$$

One idea is to solve the Lagrangian of equation (2.2) using a proximal minimization algorithm. However there is no closed form for the proximal operator with the $L_{1,\infty}$ norm. Another idea is to directly solve the constrained optimization problem using a gradient projection descent algorithm. In this case, the projection to an $L_1$ norm ball can be implemented efficiently, while inducing the sparsity of its output (Duchi et al. (2008)).

Our gradient projection descent algorithm can be implemented as a variation of any gradient descent method, as shown in Algorithm 1. In each iteration of the original gradient descent method, we project its output to the sparse DNN function class using Algorithm 2. Note that the uniform convergence of the empirical risk to the true risk holds for any hypothesis defined in Theorems 2 and 3. Therefore, it also applies to the gradient projection descent algorithm output.

## 5. Numerical Results

In this section, we validate our theorem using both simulated and real-data experiments. We first design two synthetic experiments to demonstrate the theoretical advantage of sparse DNNs. In paritcular, we illustrate the power of $L_{1,\infty}$-weight normalization for high-dimensional problems. Furthermore, we apply our algorithm to convolutional layers, and validate our theoretical findings on CIFAR-10 data sets. For each setting, we measure the training error, generalization error, test accuracy, and model sparsity in order to demonstrate the influence of $c$ on the generalization ability and the sparsity of the model. Recall that the generalization error is the difference between the training error and the test error. Note that we do not have access to the underlying distribution of the input $x$ and the output $y$. Thus, the generalization error refers to the empirical loss on the test set in all experiments. Furthermore, the test accuracy is the classification accuracy for the test data. The sparsity rate is the ratio of the number of zero parameter estimates to the size of the weight matrices. In this section, we use the format $d_0 - d_1 - \cdots - d_{k+1}$ to define the architecture of a neural network, where $k$ is the number of hidden layers, $d_0$ is the input dimension, $d_{k+1}$ is the output dimension, and $d_i$ denotes the number of neurons in the $i$th hidden layer.

Table 1. Training error, test error, generalization error, and model sparsity for the regression experiment.

| | train err | test err | gen err | sparsity % |
|---|---|---|---|---|
| $c = \infty$ | 0.000 | 69.520 | 69.520 | 3.02% |
| $c = 10.00$ | 0.000 | 35.571 | 35.571 | 41.58% |
| $c = 2.00$ | 0.052 | 8.129 | 8.077 | 61.42% |
| $c = 1.00$ | 0.131 | 2.424 | 2.426 | 84.69% |
| $c = 0.90$ | 0.173 | 2.424 | 2.251 | 87.62% |
| $c = 0.80$ | 0.197 | 2.384 | 2.186 | 89.80% |
| $c = 0.70$ | 0.235 | 2.334 | 2.099 | 91.09% |
| $c = 0.60$ | 0.252 | 2.247 | 1.994 | 91.78% |
| $c = 0.50$ | 0.286 | 2.140 | 1.854 | 93.33% |
| $c = 0.40$ | 0.387 | 2.209 | 1.822 | 93.88% |
| $c = 0.30$ | 0.850 | 2.526 | 1.675 | 94.18% |

### 5.1. The regression experiment

We evaluate our algorithm on a high-dimensional linear regression problem $y = \boldsymbol{x}^T\boldsymbol{\beta} + \varepsilon$, where the coefficient $\boldsymbol{\beta}$ is a sparse vector. We sample 500 random samples $(\boldsymbol{x}_i, y_i) \in \mathbb{R}^{1000} \times \mathbb{R}, i = 1, \ldots, 500$ for training, and 1,500 samples for testing from the distribution below.

1. Generate the coefficient $\boldsymbol{\beta}$ by $\beta_i \sim \text{Unif}(0.15, 150)$, for $i = 1, \ldots, 100$, setting the rest of $\boldsymbol{\beta}$ to zero.

2. For $\forall i$, first independently sample an auxiliary variable $\mathbf{z}_i \in \mathbb{R}^{1000}$ from $N(\mathbf{0}, \boldsymbol{I})$. Then, generate $\boldsymbol{x}_i$ by $x_{i1} = z_{i1}$, and $x_{ij} = z_{ij} + 0.2(z_{i,j+1} + z_{i,j-1})$, for $j = 2, \ldots, 1000$. Finally, sample $y_i$ from $N(\boldsymbol{x}_i^T\boldsymbol{\beta}, 1)$

Note that we make the high-dimensional problem more challenging in the presence of multicollinearity. We train the model with one fully connected layer and 300 output units using ReLU, and the loss function is the mean square error. We summarize the results in Table 1, which are estimated using the mean of 10 repeated trials.

As shown in Figure 1a and Figure 1b, as $c$ increases, the weight matrices become denser and the generalization error increases, which matches the conclusion of Theorem 2.

When $c = \infty$, or equivalently with no regularization, the model fits the training data perfectly, suffering from serious overfitting. This problem can be solved by applying $L_{1,\infty}$ weight normalization with a proper $c$, because the test error decreases by more than 95% if set $c = 1$.

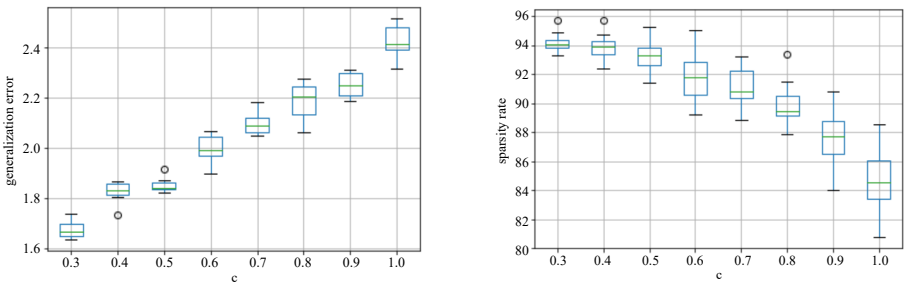


(a) Generalization error vs. $c$.

(b) Sparsity rate vs. $c$.

Figure 1. Box plots of the generalization error and sparsity rate for different $c$ in the regression experiment.

Table 2. Training error, generalization error, test accuracy, and model sparsity for the classification experiment.

| | train err | gen err | test acc(%) | sparsity(%) |
|---|---|---|---|---|
| $c = \infty$ | 0.005 | 0.543 | 71.60 | 2.39 |
| $c = 1.00$ | 0.016 | 0.624 | 83.50 | 66.71 |
| $c = 0.50$ | 0.087 | 0.337 | 87.30 | 68.43 |
| $c = 0.30$ | 0.053 | 0.297 | 88.40 | 90.78 |
| $c = 0.22$ | 0.034 | 0.280 | 88.93 | 93.29 |
| $c = 0.19$ | 0.046 | 0.273 | 89.10 | 94.53 |
| $c = 0.16$ | 0.030 | 0.250 | 89.23 | 95.40 |
| $c = 0.13$ | 0.077 | 0.177 | 89.93 | 96.60 |
| $c = 0.10$ | 0.121 | 0.155 | 90.01 | 97.53 |
| $c = 0.07$ | 0.207 | 0.102 | 90.12 | 98.98 |
| $c = 0.04$ | 0.239 | 0.112 | 89.57 | 99.04 |
| $c = 0.01$ | 0.265 | 0.068 | 88.48 | 99.49 |

### 5.2. The classification experiment

We first consider a high-dimensional nonlinear binary classification problem. We sample 500 random samples $(\boldsymbol{x}_i, y_i) \in \mathbb{R}^{500} \times \{0, 1\}, i = 1, \ldots, 500$, for training, and 1,000 samples for testing from the distribution below:

1. Generate $\alpha \sim N(0, 1)$.

2. For $\forall i$, independently sample $x_{ij}$, the $j$th element of $\boldsymbol{x}_i$, from $N(\alpha/2, 1/4)$, for $j = 1, \ldots, 500$, and

$$y_i = \begin{cases} 1, e^{x_{i1}} + x_{i2}^2 + 5\sin(x_{i3}x_{i4}) - 3 > 0 \\ 0, \text{otherwise} \end{cases}.$$

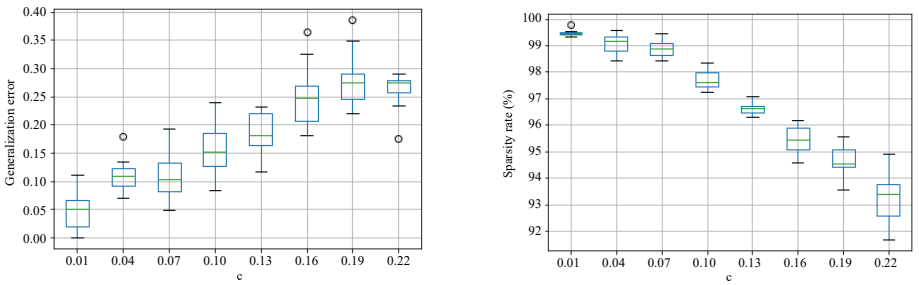


(a) Generalization error vs. $c$.

(b) Sparsity rate vs. $c$.

Figure 2. Box plots of the generalization error and sparsity rate for different $c$ in the classification experiment.

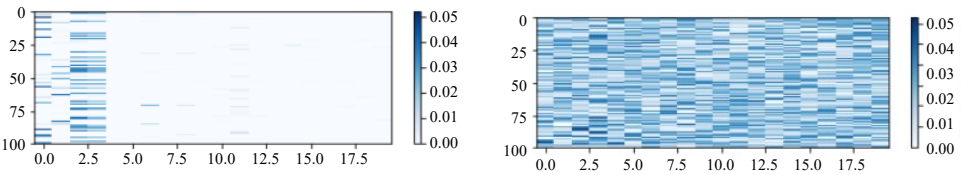


(a) $L_{1,\infty}$-weight normalization with $c = 0.07$.

(b) With no regularization.

Figure 3. Visualization of the first 20 columns of the resulting weight matrix representing the first hidden layer with/without $L_{1,\infty}$-weight normalization.

We use a 500-100-50-20-2 fully connected neural network with ReLU, and the loss function is cross entropy. We report the results in Table 2, which are estimated using the mean of 10 repeated trials.

As illustrated in Figure 2a, the generalization error decreases as $c$ decreases, which matches the conclusion of Theorem 3. Furthermore, the network becomes sparser with a smaller $c$, which is evident in Figure 2b. However, there is a trade-off between approximation and generalization ability. A smaller $c$ leads to a smaller generalization error. On the other hand, a small $c$ limits the expressive power of the neural network. For example, decreasing $c$ from 0.10 to 0.07 nearly doubles the training error.

With no regularization, the model fits the training data perfectly, but performs poorly on the test data set. We can improve the test accuracy by more than 20% using $L_{1,\infty}$ weight normalization with $c = 0.07$, while the resulting weight matrix is much sparser, as shown in Figure 3. We also observe that the first four columns of the resulting weight matrix are dense, while the others are sparse. This is because only the first four elements of the input are included in the true model.

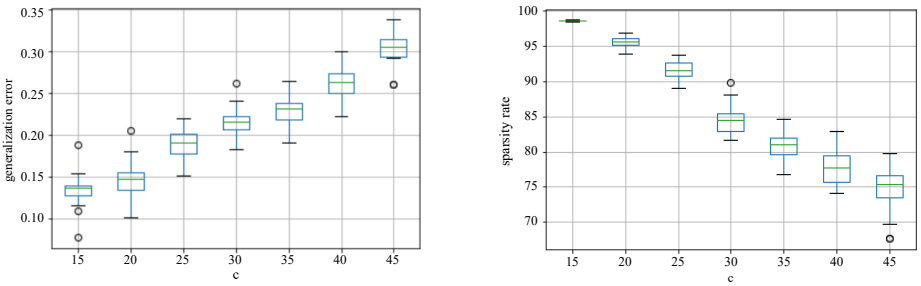


(a) Generalization error vs. $c$.

(b) Sparsity rate vs. $c$.

Figure 4. Box plots of generalization error and sparsity rate for different $c$ in the CIFAR-10 experiment.

### 5.3. CIFAR-10

We extend our method to CNNs in the second experiment. CIFAR-10 (Krizhevsky (2009)) consists of 60,000 $32 \times 32$ color images in 10 classes. A small kernel size assumes local sparsity; thus, it is not necessary to apply $L_{1,\infty}$ weight normalization to convolutional layers with small kernel sizes. We use a modified VGG-16 to train the model, where the first two $3 \times 3$ convolutional layers are replaced by two $21 \times 21$ convolutional layers. Note that VGG-16 is the CNN model proposed by Simonyan and Zisserman (2015). We perform 20-fold cross-validation to test the models' ability to predict new data.

As shown in Figure 4b, when $c$ increases, the network becomes denser. For example, when $c = 15$, the connection is very sparse, because more than 95% of its elements are learned to be zero. However, if we increase $c$ from 15 to 45, the sparsity rate reduces by almost 25%. Furthermore, Figure 4a indicates that picking a larger $c$ might result in poorer generalization. For instance, the generalization error doubles when $c$ is increased from 15 to 45. These observations match the conclusion of Theorem 3.

### 5.4. Selection of the normalization constant

The optimal normalization constant is chosen using $k$-fold cross-validation (Kohavi (1995); Tou and Gonzalez (1974)).

We give examples of selecting $c$ for the regression and classification problems in Sections 5.1 and 5.2, respectively. As shown in Figure 5, we plot the average cross-validation score against the normalization constant $c$ in both experiments. Then, we choose the optimal $c$ that corresponds to the largest average cross-validation score.

Table 3. Comparison of different regularizations on the previous classification experiment, MNIST, and CIFAR10. The bold results are the best two methods in each experiment.

| Regularizer | Cla. Exp | MNIST | CIFAR10 |
|---|---|---|---|
| No | 71.6 | 97.85 | 93.34 |
| $L_1$, $\lambda = 0.1$ | 50.0 | 13.87 | 48.32 |
| $L_1$, $\lambda = 0.01$ | 50.0 | 11.35 | 92.53 |
| $L_1$, $\lambda = 0.001$ | **81.6** | 97.33 | 93.43 |
| $L_1$, $\lambda = 0.0001$ | 73.2 | 97.99 | 93.64 |
| $L_2$, $\lambda = 0.1$ | 70.8 | 80.30 | 80.41 |
| $L_2$, $\lambda = 0.01$ | 73.4 | 92.30 | 90.38 |
| $L_2$, $\lambda = 0.001$ | 73.2 | 94.43 | 91.41 |
| $L_2$, $\lambda = 0.0001$ | 71.8 | 97.90 | **93.72** |
| Dropout, $r_d = 0.5$ | 73.5 | **98.11** | 93.42 |
| Our Approach | **91.0** | **98.03** | **93.75** |

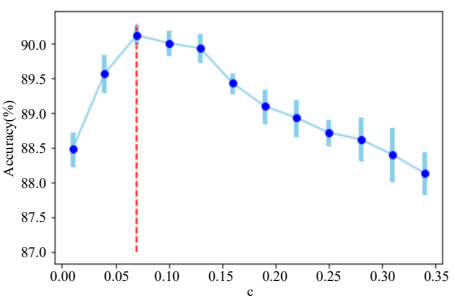


(a) Accuracy on test data set vs. $c$ in the classification experiment.

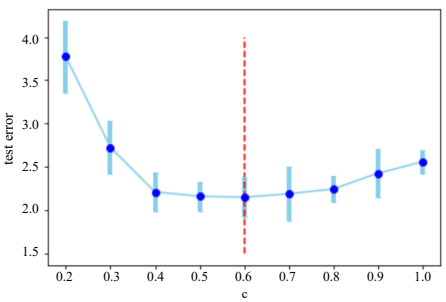


(b) Test error vs. $c$ in the regression experiment.

Figure 5. Examples of the selection of $c$.

### 5.5. Comparison with other regularizers

While establishing strong theoretical foundations for $L_{1,\infty}$ weight normalization, we show that our method performs well in practice by comparing its performance with that of popular regularization techniques, including $L_1$, $L_2$ (weight decay), and dropout regularizations, on the previous classification example, MNIST, and CIFAR-10 in terms of their classification accuracy. These additional experiments are not intended to show the supremacy of well-tuned neural network architectures, but rather to illustrate the comparative performance of the $L_{1,\infty}$ weight normalization against that of other regularization methods via a fair comparison. Therefore, we use simple architectures for demonstration. In the MNIST experiment, the input image is resized to $784 \times 1$, and then passed to a 900-10 fully connected neural network with ReLU. The loss function is cross

entropy.

By using $L_1$ regularization with the hyperparameter $\lambda$, a penalty term $\lambda \sum \|\mathbf{W}\|_{1,1}$ is added to the original loss function, where $\mathbf{W}$ is the weight matrix. By implementing $L_2$ regularization with the hyperparameter $\lambda$, a penalty term $\lambda \sum \|\mathbf{W}\|_{2,2}^2 /2$ is added to the original loss function. For each experiment, we compare different regularizers with various hyperparameters using the same baseline model to ensure a fair comparison. We show in Table 3 that our method is competitive with other methods with common regularizers.

## 6. Conclusion

We have developed a systematic framework for sparse DNNs using $L_{1,\infty}$ weight normalization. We have established the Rademacher complexity of the related sparse DNN space. Based on this result, we have derived generalization error bounds for both regression and classification. The easily implemented gradient projection descent algorithm allows us to obtain a sparse DNN in practice. In experiments, we have shown that the proposed $L_{1,\infty}$ minimization process leads to neural network sparsification that is competitive with current approaches, while empirically validating our theoretical findings.

We have so far used a single $c$ to control the sparsity of the network. It would be interesting to extend the current framework to a network in which $c$ varies by layer. This poses additional challenges for the computation in terms of tuning the hyperparameters. In other research, we are trying to use Bayesian optimization (Shahriari et al. (2016)) to automatically select these hyperparameters.

## Supplementary Material

The online Supplementary Material provides proofs of the three main theorems and the technical lemmas used to prove these theorems. In addition, we extend the classification experiment in Section 5.2 to examine the effects of sample size and depth on generalization. Finally, we show using an experiment that the projection gradient descent algorithm is not sensitive to the initial step size.

## Acknowledgments

The research of Zhouwang Yang was supported by the NSF of China (No. 11871447) and the Anhui Initiative in Quantum Information Technologies (AHY150200). The research of Xiao Wang was supported by the US National Science Foundation. We gratefully acknowledge the support of NVIDIA Corporation with the donation of the Titan Xp used for this research.

## References


Bartlett, P. L. (1998). The sample complexity of pattern classification with neural networks: The size of the weights is more important than the size of the network. *IEEE Transactions on Information Theory* **44**, 525–536.

Duchi, J., Shalev-Shwartz, S., Singer, Y. and Chandra, T. (2008). Efficient projections onto the l 1-ball for learning in high dimensions. In *Proceedings of the 25th International Conference on Machine Learning*, 272–279. Association for Computing Machinery, New York.

Golowich, N., Rakhlin, A. and Shamir, O. (2018). Size-independent sample complexity of neural networks. In *Proceedings of the 31st Conference on Learning Theory* **PMLR 75**, 297–299.

Goodfellow, I., Bengio, Y., Courville, A. and Bengio, Y. (2016). *Deep Learning*. Volume 1. MIT Press, Cambridge.

Han, S., Mao, H. and Dally, W. J. (2016). Deep compression: Compressing deep neural networks with pruning, trained quantization and huffman coding. In *Proceedings of the 4th International Conference on Learning Representations*.

Jaderberg, M., Simonyan, K., Zisserman and Kavukcuoglu, K. (2015). Spatial transformer networks. In *Advances in Neural Information Processing Systems* **28** (Edited by C. Cortes, N. D. Lawrence, D. D. Lee, M. Sugiyama and R. Garnett), 2017–2025. Curran Associates, Inc.

Kohavi, R. (1995). A study of cross-validation and bootstrap for accuracy estimation and model selection. In *Proceedings of the International Joint Conference on Artificial Intelligence*, 1137–1145. Montreal, Canada.

Krizhevsky, A. (2009). *Learning Multiple Layers of Features from Tiny Images*. Technical report. University of Toronto.

Krizhevsky, A., Sutskever, I. and Hinton, G. E. (2012). Imagenet classification with deep convolutional neural networks. In *Advances in Neural Information Processing Systems* **25** (Edited by F. Pereira, C.J.C. Burges, L. Bottou and K.Q. Weinberger), 1097–1105.

Louizos, C., Ullrich, K. and Welling, M. (2017). Bayesian compression for deep learning. In *Advances in Neural Information Processing Systems* **30** (Edited by I. Guyon, U.V. Luxburg, S. Bengio, H. Wallach, R. Fergus, S. Vishwanathan and R. Garnett), 3288–3298.

Louizos, C., Welling, M. and Kingma, D. P. (2018). Learning sparse neural networks through $l_0$ regularization. In *Proceedings of the International Conference on Learning Representations. arXiv:1712.01312.*

Mohri, M., Rostamizadeh, A. and Talwalkar, A. (2012). *Foundations of Machine Learning*. MIT Press.

Molchanov, D., Ashukha, A. and Vetrov, D. P. (2017). Variational dropout sparsifies deep neural networks. In *International Conference on Machine Learning*.

Neyshabur, B., Tomioka, R. and Srebro, N. (2015). Norm-based capacity control in neural networks. In *Proceedings of the 28th Conference on Learning Theory* **PMLR 40**, 1376–1401.

Nowlan, S. J. and Hinton, G. E. (1992). Simplifying neural networks by soft weight-sharing. *Neural Computation* **4**, 473–493.

Salimans, T. and Kingma, D. P. (2016). Weight normalization: A simple reparameterization to accelerate training of deep neural networks. In *Advances in Neural Information Processing Systems* **29** (Edited by D.D. Lee, M. Sugiyama, U.V. Luxburg, I. Guyon and R. Garnett), 901–909.

Shahriari, B., Swersky, K., Wang, Z., Adams, R. P. and De Freitas, N. (2016). Taking the human

out of the loop: A review of bayesian optimization. In *Proceedings of the IEEE* **104**, 148–175.

Simonyan, K. and Zisserman, A. (2015). Very deep convolutional networks for large-scale image recognition. In *Proceedings of the International Conference on Learning Representations. arXiv:1409.1556*.

Srinivas, S., Subramanya, A. and Babu, R. V. (2017). Training sparse neural networks. In *2017 IEEE Conference on Computer Vision and Pattern Recognition Workshops (CVPRW)* **1**, 455–462. IEEE.

Srivastava, N., Hinton, G., Krizhevsky, A., Sutskever, I. and Salakhutdinov, R. (2014). Dropout: A simple way to prevent neural networks from overfitting. *Journal of Machine Learning Research* **15**, 1929–1958.

Sun, S., Chen, W., Wang, L., Liu, X. and Liu, T.-Y. (2016). On the depth of deep neural networks: A theoretical view. In *Proceedings of the 30th AAAI Conference on Artificial Intelligence*, 2066–2072.

Szegedy, C., Liu, W., Jia, Y., Sermanet, P., Reed, S., Anguelov, D. et al. (2015). Going deeper with convolutions. In *Proceedings of the IEEE Conference on Computer Vision and Pattern Recognition*, 1–9.

Tou, J. T. and Gonzalez, R. C. (1974). *Pattern Recognition Principles*.

Ming Wen

School of Mathematical Sciences, University of Science and Technology of China, China.

E-mail: mosqwen@mail.ustc.edu.cn

Yixi Xu

Department of Statistics, Purdue University, West Lafayette, IN 47907, USA.

E-mail: xu573@purdue.edu

Yunling Zheng

School of Gifted Young, University of Science and Technology of China, China.

E-mail: zyunling@mail.ustc.edu.cn

Zhouwang Yang

School of Mathematical Sciences, University of Science and Technology of China, China.

E-mail: yangzw@ustc.edu.cn

Xiao Wang

Department of Statistics, Purdue University, West Lafayette, IN 47907, USA.

E-mail: wangxiao@purdue.edu

(Received November 2018; accepted October 2019)